

1     **Molecular and morphological analyses clarify species delimitation and reveal a**  
2                                    **new *Betula* species in section *Costatae***

3     Luwei Wang<sup>1,2#</sup>, Junyi Ding<sup>1,2#</sup>, James S. Borrell<sup>3</sup>, Hugh A. McAllister<sup>4</sup>, Feifei  
4     Wang<sup>1,2</sup>, Lu Liu<sup>1,2</sup>, Nian Wang<sup>1,2,5\*</sup>

5     <sup>1</sup>State Forestry and Grassland Administration Key Laboratory of Silviculture in  
6     downstream areas of the Yellow River, College of Forestry, Shandong Agricultural  
7     University, Tai'an 271018, China.

8     <sup>2</sup>Mountain Tai Forest Ecosystem Research Station of State Forestry and Grassland  
9     Administration, College of Forestry, Shandong Agricultural University, Tai'an 271018,  
10    China.

11    <sup>3</sup>Natural Capital and Plant Health Department, Royal Botanic Gardens Kew,  
12    Richmond, Surrey TW9 3AB, UK.

13    <sup>4</sup>School of Life Sciences, Biosciences Building, University of Liverpool, Crown  
14    Street, Liverpool L69 7ZB, UK.

15    <sup>5</sup>State Key Laboratory of Crop Biology, Shandong Agricultural University, Tai'an  
16    271018, Shandong province, China

17    **Running title:** species delimitation and a new *Betula* species in section *Costatae*

18    <sup>#</sup>contributed equally to this work

19

20    \*For correspondence.

21    Email: [nian.wang@sdau.edu.cn](mailto:nian.wang@sdau.edu.cn)

22

23

24 **Background and Aims** Delineating closely related and morphologically similar  
25 species with overlapping ranges can be difficult. Here, we use section *Costatae* (genus  
26 *Betula*) as a model to resolve species and subspecies boundaries in four  
27 morphologically similar trees: *Betula ashburneri*, *Betula costata*, *Betula ermanii* and  
28 *Betula utilis* (including ssp. *utilis*, and diploid and tetraploid races of ssp.  
29 *albosinensis*).

30 **Methods** We genotyped 298 individuals (20-80 per species) from 38 populations at 15  
31 microsatellite markers and a subset of 34 individuals from 21 populations using  
32 restriction-site associated DNA sequencing (RAD-seq). Morphometric analysis was  
33 conducted to characterise leaf variation for a subset of 89 individuals.

34 **Key Results** Molecular analyses and leaf morphology found little differentiation  
35 between *B. ashburneri*, diploid *B. utilis* ssp. *albosinensis* and some samples of *B.*  
36 *utilis* ssp. *utilis* suggesting that these should be treated as a single species. By contrast,  
37 tetraploid *Betula utilis* ssp. *albosinensis* was divided into two groups with group I  
38 genetically similar to *B. utilis* ssp. *utilis* based on SNPs and group II, a very distinct  
39 cluster, which we propose as a new species, namely, *Betula buggsii*. Phylogenomic  
40 analysis based on 2,285,620 SNPs show a well-supported monophyletic clade of *B.*  
41 *buggsii*, forming a sister with a well-supported clade of *B. ashburneri*, diploid *B.*  
42 *albosinensis* and some samples of *B. utilis* ssp. *utilis*. Morphologically, *Betula buggsii*  
43 is characterised by elongated lenticels and a distinct pattern of bark peeling. *Betula*  
44 *buggsii* is geographically restricted to the Qinling-Daba Mountains.

45 **Conclusions** Our study reveals six genetically distinguishable species: *B. ashburneri*,

46 *B. bugssii*, *B. costata*, *B. utilis* ssp. *utilis*, *B. utilis* ssp. *albosinensis* and *B. ermanii*.

47 Our research demonstrates an integrative approach in delimitating species using

48 morphological and genetic samples from their nearly entire distributions. Analyses

49 based on subsets of species' distributions may lead to erroneous species or subspecies

50 delineation.

51 **Keywords:** birch, cryptic species, microsatellite markers, polyploidy, RAD-seq,

52 species delineation

53

54 **INTRODUCTION**

55 Species delineation based on morphology may be confounded by intra-specific  
56 variation among populations and limited differentiation between closely-related  
57 species (Whittall et al., 2004; Leliaert et al., 2009; Wang et al., 2014b; Lissambou et  
58 al., 2019). Where species co-occur, this may be further exacerbated by introgression  
59 and hybridisation (Bacon et al., 2012; Andújar et al., 2014), or may be  
60 morphologically impossible due to cryptic speciation (Bickford et al., 2007; Fišer et  
61 al., 2018). Despite advances in phylogenetic methods, this has meant that many  
62 species rich genera have remained unresolved, hindering our understanding of species  
63 ecology and evolution as well as limiting our ability to deliver effective conservation  
64 management.

65 *Betula* L. (Betulaceae) is such a genus with many taxonomic issues. The genus  
66 consists of approximately 65 species and subspecies (Ashburner & McAllister, 2016)  
67 with some spanning a very broad latitudinal and longitudinal range, such as *B.*  
68 *platyphylla*, ranging from Europe to eastern Asia and from the Himalayas to Siberia.  
69 Species such as *B. michauxii* and *B. nana*, are morphologically convergent but  
70 comparatively distantly-related (Wang et al., 2016; Wang et al., 2020), having evolved  
71 independently in North America and Scotland respectively. Analysis of *Betula*  
72 taxonomy is complicated by these broad ranges, frequent inter-specific hybridisation  
73 (Anamthawat-Jónsson & Tómasson, 1999; Wang et al., 2014a; Zohren et al., 2016;  
74 Tsuda et al., 2017), polyploidy and considerable morphological variation (Wang et al.,  
75 2014b; Ashburner & McAllister, 2016).

76 Where ranges overlap, introgression appears frequent between species of the same  
77 ploidy level (Nagamitsu et al., 2006; Ashburner & McAllister, 2016) and even  
78 differing ploidy levels (Anamthawat-Jónsson & Thórsson, 2003; Wang et al., 2014a;  
79 Zohren et al., 2016; Tsuda et al., 2017). *Betula* species from different subgenera  
80 appear able to hybridise readily, such as hybridisation between *B. alleghanensis* and *B.*  
81 *papyrifera* (Thomson et al., 2015). Polyploidy is also common within *Betula*,  
82 accounting for nearly 60% of the described taxa, ranging from diploid to dodecaploidy,  
83 with cytotypes observed for some species, such as *B. chinensis* (6x and 8x)  
84 (Ashburner & McAllister, 2016).

85 In this study, we use section *Costatae* as a model in which to demonstrate combined  
86 morphological and genetic methods to resolve these taxonomic issues (Table 1).  
87 Section *Costatae* includes the diploids *B. ashburneri* and *B. costata*, with *B.*  
88 *ashburneri* discovered from south-east Tibet and reported to have distributions in  
89 north-west Yunnan and western Sichuan (McAllister & Rushforth, 2011) and with *B.*  
90 *costata* distributed in northern and northeastern China, Japan and Russian Far East  
91 (Ashburner & McAllister, 2016). Section *Costatae* also includes two tetraploids: *B.*  
92 *utilis* (subdivided into ssp. *utilis* and ssp. *albosinensis*) occurring from the Himalayas  
93 to north China without clear geographical and morphological intra-specific boundaries  
94 and *B. ermanii* from northeastern China, Japan and Russian Far East. Several varieties  
95 of these tetraploid species have also been named based on a limited number of  
96 herbarium specimens, such as *B. utilis* var. *prattii*, *B. albosinensis* var. *septentrionalis*  
97 and *B. ermanii* var. *lanata* (Ashburner & McAllister, 2016), though their taxonomic

98 validity is unclear.

99 Confusingly, *B. utilis* ssp. *utilis* was described to have distributions in Gansu, Ningxia,  
100 Qinghai and Shaanxi according to Flora of China (Li & Skvortsov, 1999), where *B.*  
101 *utilis* ssp. *utilis* was not recorded in Ashburner and McAllister's monograph  
102 (Ashburner & McAllister, 2016) (Table 1). Recently, a 'diploid' *B. albosinensis* has  
103 been discovered from the Qinling Mountains in central China (Hu et al., 2019). A  
104 phylogenetic tree based on the internal transcribed spacer (ITS) region indicated a  
105 close relationship between the 'diploid' *B. albosinensis*, *B. ashburneri* and *B. costata*  
106 (Hu et al., 2019).

107 It remains unknown if the 'diploid' *B. albosinensis*, *B. ashburneri* and *B. costata*  
108 represent distinct genetic entities. Moreover, it remains unknown if the tetraploids *B.*  
109 *utilis* ssp. *albosinensis*, *B. ermanii* and *B. utilis* ssp. *utilis* described in Flora of China  
110 and in Ashburner and McAllister's monograph, respectively, represent distinct genetic  
111 entities (Li & Skvortsov, 1999; Ashburner & McAllister, 2016). For ease of reference,  
112 we abbreviate the 'diploid' *B. albosinensis* and *B. utilis* ssp. *utilis* described in  
113 Ashburner and McAllister's monograph and in Flora of China as *B. albosinensis*  
114 [DA], *B. utilis* [AM] and *B. utilis* [FC], respectively.

115 To resolve taxonomic issues within section *Costatae*, we carried out morphological  
116 analysis, microsatellite genotyping and restriction-site associated DNA sequencing  
117 (RAD-seq). Our specific aims are to (1) identify the number of distinct genetic groups  
118 within section *Costatae*, with particular attention to (2) resolving the phylogenetic  
119 position of *B. utilis* [FC] and *B. albosinensis* [DA]; finally, (3) we integrate genetic

120 data with morphology and geographic distributions to present a revised treatment of  
121 species boundaries within section *Costatae*. We consider the applicability of this  
122 approach to other taxonomically complex genera.

123

## 124 **Materials and methods**

### 125 **Sampling**

126 Samples putatively identified (based on morphology) as *B. utilis* [AM], *B. utilis* ssp.  
127 *albosinensis*, *B. ermanii*, *B. albosinensis* [DA], *B. utilis* [FC] and *B. costata* were  
128 collected from between three and twelve populations each (Fig. 1). All species were  
129 collected from naturally occurring woodland, meaning that they were not artificially  
130 planted. Leaf samples were collected between May and September of 2018 and 2019,  
131 with each sample separated by ~20m. A herbarium specimen was created for each  
132 sample except for a subset of samples where branches were difficult to obtain. For  
133 these samples, cambium tissue was collected. A GPS system (UniStrong) was used to  
134 record the coordinate points of each population. Detailed species and population  
135 sampling information is provided in Supplementary Data Table S1.

### 136 **Species identification**

137 *Betula utilis* [AM] is distributed through SE Tibet to Yunnan and Sichuan and *B. utilis*  
138 ssp. *albosinensis* occurs in North Sichuan, Hubei, Shaanxi, Shanxi, Henan and Hebei  
139 (Ashburner and McAllister, 2016). These two species co-occur in Sichuan province.  
140 Due to a morphological continuum between *B. utilis* [AM] and *B. utilis* ssp.  
141 *albosinensis*, we assigned our populations based on geographic origins, with

142 populations from northwestern Yunnan designated as *B. utilis* [AM] and populations  
143 from south Shaanxi, Hubei, Shanxi, Henan and Hebei designated as *B. utilis* ssp.  
144 *albosinensis*. *Betula utilis* [FC] occupies a higher altitude than *B. utilis* ssp.  
145 *albosinensis* and can be distinguished from the latter by its leathery dark green leaves  
146 (Ashburner & McAllister, 2016; Li & Skvortsov, 1999). *Betula costata* and *B. ermanii*,  
147 having distributions in northeastern China, can be distinguished from leaf morphology  
148 with the former having lanceolate leaves and the latter triangular-ovate leaves (Li &  
149 Skvortsov, 1999; Ashburner & McAllister, 2016).

#### 150 **Morphometric analyses**

151 For analyses of leaf shape among these species, we selected 6-27 individuals per taxa  
152 and sampled 283 leaves. Leaves were scanned individually using a Hewlett-Packard  
153 printer (LaserJet Pro MFP M128fn) with a resolution of 600 dpi. Thirteen landmarks  
154 were selected from each scanned leaf according to the protocols of (Liu et al., 2018;  
155 Hu et al., 2019). The 13 landmarks were converted to a configuration of 26 cartesian  
156 coordinates using ImageJ (Abràmoff et al., 2004). A Generalized Procrustes Analysis  
157 (GPA) was performed using the procGPA function in the R package “shapes” (Dryden,  
158 2019). Eigenleaves were visualized using the “shapepca” function and principal  
159 component scores, percentage variance and Procrustes-adjusted coordinates were  
160 obtained from procGPA object values.

#### 161 **DNA extraction and microsatellite genotyping**

162 High quality DNA was extracted from cambial tissues following a modified 2x CTAB  
163 (cetyltrimethylammonium bromide) protocol (Wang et al., 2013). Extracted DNA was



164 assessed with 1.0% agarose gels. Fifteen microsatellite loci developed for *B.*  
165 *platyphylla* var. *japonica* (Wu et al., 2002), *B. pendula* (Kulju et al., 2004), *B.*  
166 *pubescens* ssp. *tortuosa* (Truong et al., 2005) and *B. maximowicziana* (Tsuda et al.,  
167 2009) were used to genotype our samples (Supplementary Data, Table S2), with the 5'  
168 terminus of the forward primers labeled with FAM, HEX or TAM fluorescent probes.  
169 These microsatellite loci have a good cross compatibility in multiple *Betula* species.  
170 Each microsatellite locus was amplified individually and was artificially combined  
171 into four multiplexes. The PCR protocol followed Hu et al. (2019). Microsatellite  
172 alleles were scored using GENEMARKER 2.4.0 (Softgenetics) and checked manually.  
173 Individuals with more than three missing loci were excluded for further analyses,  
174 resulting in 298 individuals in the final dataset.

#### 175 **RAD-seq**

176 A subset of 34 DNA samples were selected for RAD-seq using an Illumina HiSeq  
177 2500 and 150-bp pair-end sequencing with the restriction enzyme *PstI* (Personalbio  
178 company, Shanghai, China). These were combined with eight additional samples of  
179 section *Costatae* previously sequenced, using the same restriction enzyme in Wang et  
180 al. (2020). These samples represented six *B. costata*, six *B. utilis* [AM], six *B. ermanii*,  
181 twelve *B. utilis* ssp. *albosinensis*, seven *B. utilis* [FC] and one of each of *B.*  
182 *albosinensis* [DA], *B. ashburneri*, *B. ermanii* var. *lanata*, *B. albosinensis* var.  
183 *septentrionalis*, and *B. utilis* var. *prattii* (Supplementary Data, Table S3). The raw data  
184 were trimmed using Trimmomatic (Bolger et al., 2014) in paired-end mode. Reads  
185 with a quality of below 20 within the sliding-window of 5 bp and unpaired reads were

186 discarded. We performed LEADING and TRAILING to remove bases with a quality  
187 below 20. Then we performed a SLIDINGWINDOW step to discard reads shorter  
188 than 40 bp. Filtered reads of each sample were aligned to the whole genome sequence  
189 of *B. pendula* (Salojärvi et al., 2017) using BWA-MEM v.0.7.17-r1188 algorithm in  
190 BWA (v0.7.17) with default parameters (Li & Durbin, 2009). Non-specific mapped  
191 reads were discarded. All subsequent analyses were performed using SAMtools v1.8  
192 (Li et al., 2009) and GATK V4.1.4 (McKenna et al., 2010; DePristo et al., 2011).  
193 These include conversion of alignments into indexed binary alignment map (BAM)  
194 files, marking duplicates, calling genotypes and filtering SNPs (McKenna et al., 2010;  
195 DePristo et al., 2011). SNPs within a 50 kb window with  $r^2 > 0.5$  and a minimum  
196 allele frequency (MAF)  $< 0.01$  were removed to reduce linkage disequilibrium using  
197 BCFtools v1.10.2 (Li, 2011). Prior to population structure analysis, we retained only  
198 sites with no missing data, resulting in 82,137 SNPs for downstream analyses.

#### 199 **Analyses of microsatellite data and SNPs**

200 A principal coordinate analysis (PCoA) was performed on microsatellite data of *B.*  
201 *utilis* [AM], *B. utilis* [FC], *B. utilis* ssp. *albosinensis*, *B. albosinensis* [DA], *B. costata*  
202 and *B. ermanii* using POLYSAT (Clark & Jasieniuk, 2011) implemented in R 4.0.2 (R  
203 Core Team, 2020), based on Bruvo's genetic distances (Bruvo et al., 2004). For  
204 nucleotide SNPs, a principal component analysis (PCA) was carried out using the  
205 'adegenet' R package 2.1.1 (Jombart, 2008).

206 Microsatellite data were analyzed in STRUCTURE (Pritchard et al., 2000) to identify  
207 the most likely number of genetic clusters (K) with a ploidy of four. Ten replicates

208 were performed with 1,000,000 iterations and a burn-in of 100,000 for each run at  
209 each value of K from 1 to 8. We used the admixture model, with an assumption of  
210 correlated allele frequencies among populations. Individuals were assigned to clusters  
211 based on the highest membership coefficient averaged over the ten independent runs.  
212 The number of genetic clusters was estimated using the “Evanno test” (Evanno et al.,  
213 2005) implemented in Structure Harvester (Earl & vonHoldt, 2012). Replicate runs  
214 were grouped based on a symmetrical similarity coefficient of >0.9 using the Greedy  
215 algorithm in CLUMPP (Jakobsson & Rosenberg, 2007) and visualized in DISTRUCT  
216 1.1 (Rosenberg, 2004).

217 The filtered SNPs were analyzed in ADMIXTURE v1.3.0, a model-based approach to  
218 assessing population structure in a Maximum Likelihood framework (Alexander &  
219 Lange, 2011). We ran ADMIXTURE for K = 1-10 with 20 replicates for each K value  
220 and performed cross-validation error estimation in order to assess the most suitable  
221 value of K (Alexander & Lange, 2011). Replicate runs were aligned and visualised in  
222 pong v1.4.9 with the greedy algorithm (Behr et al., 2016).

### 223 **ITS and SNP based phylogenetic analyses**

224 To provide an additional line of evidence for the phylogenetic position of *B. utilis*  
225 [FC], *B. albosinensis* [DA], and *B. costata*, we generated ITS sequence and SNP  
226 based phylogenies.

227 First, we amplified the nuclear ribosomal internal transcribed spacer (nrITS) region  
228 (ITS1, 5.8S and ITS2) using primers ITS4 (White et al., 1990) and ITSLeu (Baum et  
229 al., 1998), with seven, ten, five and four individuals of *B. utilis* ssp. *albosinensis*

230 group II collected from the NSX, CKX, WLP and SNJ, respectively. The reaction mix  
231 and the PCR protocol followed that of Hu et al. (2019). PCR products were purified  
232 and sequenced at Tsingke Company (Qingdao, China). Sixty-four additional ITS  
233 sequences from Betulaceae (Wang et al., 2016) were included to infer the  
234 phylogenetic position of *B. utilis* ssp. *albosinensis* group II. In total, 90 sequences  
235 were aligned using BioEdit v7.0.9.0 (Hall, 1999) with default parameters.

236 Second, we collated RAD-seq data of 20 *Betula* taxa representing genus wide diploid  
237 species. The identity of the 20 sequenced *Betula* taxa was initially inferred via ITS  
238 sequences and genome size estimates (Wang et al., 2016). In addition, we included  
239 RAD-seq data of 17 samples generated in the present study. *Alnus inokumae* was  
240 selected as the outgroup (Supplementary Data, Table S3). SNPs of a total of 38 taxa  
241 were concatenated into a supermatrix for phylogenetic analysis. SNPs with a missing  
242 data > 50% were excluded, resulting in 2,285,620 SNPs.

243 For both the ITS alignment and the matrix of SNPs, we conducted a rapid bootstrap  
244 analysis under a GTR+GAMMA nucleotide substitution model, with 100 bootstraps  
245 and 10 searches using the maximum-likelihood method (ML) in RAxML v. 8.1.16  
246 (Stamatakis, 2006). The phylogenetic trees were visualised in FigTree v.1.3.1.

## 247 **Results**

### 248 **Morphometric analyses**

249 Landmarks were first aligned using a GPA and then a principal component analysis  
250 (PCA) was conducted to visualise the major sources of shape variance of leaves from  
251 *B. albosinensis* [DA], *B. utilis* ssp. *albosinensis*, *B. utilis* [AM], *B. utilis* [FC], *B.*

252 *costata* and *B. ermanii*. PC1 and PC2 produce largely overlapping clusters among *B.*  
253 *albosinensis* [DA], *B. utilis* ssp. *albosinensis*, *B. utilis* [AM] and *B. utilis* [FC], but *B.*  
254 *costata* and *B. ermanii* overlapped to a much lesser extent (Fig. 2a). The shape  
255 variance, represented by PC1 and PC2, is mainly influenced by leaf width and  
256 marginally influenced by leaf length (Fig. 2b).

### 257 **PCO and PCA analyses**

258 PCO analysis based on microsatellite markers revealed five clusters, with the first  
259 three axes accounting for 43.8% of the total variation (Fig. 3a). *Betula utilis* ssp.  
260 *albosinensis* forms two groups: group I overlaps substantially with *B. utilis* [AM] and  
261 *B. ermanii* whereas group II separates from all the other species on coordinate 1 (Fig.  
262 3a). *Betula utilis* [FC] and *B. albosinensis* [DA] overlap substantially whereas *B.*  
263 *costata* separates from the remaining species on coordinates 2 and 3 (Supplementary  
264 Data, Fig. S1a). *Betula ermanii* separates from *B. utilis* [AM] on coordinate 3 with *B.*  
265 *utilis* ssp. *albosinensis* group I intermediate (Supplementary Data, Fig. S1a).

266 For the sequenced individuals, between 12,234,848 and 28,155,092 reads were  
267 retained for each individual (mean 18,862,242) after trimming and filtering  
268 (Supplementary Data, Table S3). The number of variable sites of the sequenced  
269 individuals ranges from 5,520,333 to 9,735,507. A principal component analysis  
270 (PCA) based on genotype calls for 82,137 SNPs shows that both *B. utilis* ssp.  
271 *albosinensis* group II and *B. costata* separate from the remaining species and from  
272 each other (Fig. 3b). Two individuals of *B. utilis* ssp. *albosinensis* group I form a  
273 cluster and three individuals of *B. utilis* ssp. *albosinensis* group I form a cluster with

274 the previously sequenced *B. utilis* var. *prattii* and *B. albosinensis* var. *septentrionalis*  
275 (Fig. 3b). *Betula utilis* [AM] forms a cluster with the previously sequenced *B. utilis*  
276 ssp. *albosinensis* whereas *B. ermanii* and *B. ermanii* var. *lanata* form a cluster from  
277 PC1 and PC2 (Supplementary Data, Fig. S1b). *Betula albosinensis* [DA] forms a  
278 cluster with one accession of *B. utilis* [FC] whereas the remaining accessions of *B.*  
279 *utilis* [FC] form another cluster. The two individuals of *B. utilis* ssp. *albosinensis*  
280 group I position between *B. ermanii* and three individuals of *B. utilis* ssp. *albosinensis*  
281 group I. *Betula ashburneri* forms a continuum with *B. utilis* [AM] and *B. utilis* [FC]  
282 on PC1 and PC3 (Supplementary Data, Fig. S1b).

### 283 **STRUCTURE and ADMIXTURE analyses**

284 STRUCTURE analyses based on microsatellite markers identified five clusters: (1) *B.*  
285 *utilis* ssp. *albosinensis* group I, (2) *B. albosinensis* [DA] and *B. utilis* [FC], (3) *B.*  
286 *costata*, (4) *B. utilis* [AM], (5) *B. ermanii* and (6) *B. utilis* ssp. *albosinensis* group II  
287 (Supplementary Data Figs. S2-3). *B. utilis* ssp. *albosinensis* group I is genetically  
288 similar to *B. ermanii* at all K values (Fig. 4a). *Betula utilis* ssp. *albosinensis* group II  
289 includes populations SNJ, WLP, NSX and CKX and separates with the remaining  
290 species (Supplementary Data, Fig. S3). Similarly, *B. albosinensis* [DA] and *B. utilis*  
291 [FC] are genetically similar at all supported K values (Supplementary Data, Fig. S3).  
292 Admixture analysis based on the same set of SNPs showed that cross-validation error  
293 is smallest at  $K = 5$ , but only with four out of twenty replicates having an average  
294 pairwise similarity of 0.98 (Supplementary Data, Fig. S4). At the value of  $K = 6$ ,  
295 fourteen out of twenty replicates have an average pairwise similarity of 0.98. However,

296 the cross-validation error is slightly larger than that when  $K = 5$  (Supplementary Data,  
297 Fig. S4). At the value of  $K = 5$ , *B. utilis* ssp. *albosinensis* group I genetically  
298 resembles *B. utilis* [AM] with exception of samples XLA01 and XLA32, which are  
299 more genetically similar to *B. ermanii* (Fig. 4b). At the value of  $K = 6$ , *B. utilis* ssp.  
300 *albosinensis* group I separates from *B. utilis* [AM] and XLA01 and XLA32 exhibit  
301 genetic admixture from *B. ermanii* (Fig. 4b). *Betula utilis* ssp. *albosinensis* group II  
302 separates from the remaining species at the value of  $K = 3$  and onwards  
303 (Supplementary Data, Fig. S5). Interestingly, this identified that *B. albosinensis* var.  
304 *septentrionalis* and *B. utilis* var. *prattii* are genetically similar to *B. utilis* ssp.  
305 *albosinensis* group I whereas the *B. utilis* ssp. *albosinensis* and *B. utilis* ssp. *utilis* are  
306 genetically similar to *B. utilis* [AM] (Fig. 4b).

307

## 308 **Phylogenetic analyses**

### 309 **Identification of species novo *Betula buggsii***

310 Analyses of microsatellite data and SNPs indicate that *B. utilis* ssp. *albosinensis* group  
311 II is genetically distinct from other species of section *Costatae* and therefore  
312 represents a putative new species, namely *Betula buggsii*. Morphologically, despite  
313 general similarity to *B. utilis* ssp. *albosinensis*, we found *B. buggsii* is characterised by  
314 very elongated lenticels with bark peeling along lenticels into strips.

315 The phylogenetic tree based on ITS showed that *B. buggsii* samples formed a  
316 monophyletic cluster, within a clade with species of section *Acuminatae*, *B. bomiensis*  
317 and *B. nigra*. However, this clade received little support (Supplementary Data, Fig.

318 S6). The phylogenetic tree based on a matrix of 2,285,620 SNPs showed that the five  
319 individuals of *B. buggsii* from populations CKX, SNJ and WLP formed a  
320 monophyletic clade with 100% support, which was basal to a clade of *B. costata*, *B.*  
321 *ashburneri*, *B. albosinensis* [DA] and *B. utilis* [FC] (Fig. 5). The five individuals of *B.*  
322 *costata* formed a monophyletic clade whereas individuals of *B. utilis* [FC], *B.*  
323 *albosinensis* [DA] and *B. ashburneri* intermixed and together formed a monophyletic  
324 clade with 100% support (Fig. 5).

### 325 **Taxonomic treatment**

326 *Betula buggsii* N. Wang, sp. nov.

327 Diagnosis:—*Betula buggsii* is very similar with *B. utilis* ssp. *albosinensis* in leaf  
328 morphology but have very elongated lenticels on the bark of adult and elderly trees.  
329 Barks of *B. buggsii* peel along the elongated lenticels into strips. Adult or old *B. utilis*  
330 ssp. *albosinensis* trees exfoliate in large sheets (Fig. 6a). Seedlings of *B. buggsii* and *B.*  
331 *utilis* ssp. *albosinensis* (DBH < 5 cm) show no obvious difference in bark color and  
332 patterns of bark peeling.

333 Type:—CHINA. Chongqing: Chengkou County, elev. ca. 1600-2000 m, 108.7° E,  
334 31.9° N, 6 October 2018 (holotype xx; isotypes xx).

335 Distribution and habitat:—*Betula buggsii* occurs in Chongqing, western Hubei and  
336 Shaanxi with five localities discovered. *Betula buggsii* grows in mixed forests with  
337 bamboos at an altitude of between 1500 and 2100 meters. At some localities, *B.*  
338 *buggsii* grows in parapatry with *B. luminifera* but at a higher altitude. We only  
339 founded a small number of *B. buggsii* individuals within each population. Given this



340 situation, we think *B. bugssii* needs conservation.

341 Etymology:—*Betula bugssii* is named after Prof. Richard J.A. Buggs, an evolutionary  
342 biologist from the Royal Botanical Gardens Kew and Queen Mary University of  
343 London, for his devotion to research on hybridisation, phylogenetics and conservation  
344 of the genus *Betula*. The Chinese name of *B. bugssii* is “年桦” (nián huá).

345

## 346 **Discussion**

### 347 **Species delimitation within section *Costatae***

348 Here we have combined genetic, morphological and distribution data to revise species  
349 delimitation within section *Costatae* (genus *Betula*). Our results support six genetic  
350 units and thus prefer recognition of six taxa.

#### 351 **Cluster one — *B. albosinensis* [DA], *B. ashburneri* and *B. utilis* [FC].**

352 Several lines of evidence jointly support the merging of *B. albosinensis* [DA], *B.*  
353 *ashburneri* and *B. utilis* [FC]. First, PCO and STRUCTURE analyses of microsatellite  
354 markers indicate an indistinguishable cluster of *B. albosinensis* [DA] and *B. utilis* [FC]  
355 (Figs. 3a, 4a). This was further corroborated by admixture analysis of SNPs, showing  
356 an indistinguishable cluster of *B. albosinensis* [DA] and *B. utilis* [FC] (Fig. 4b).  
357 However, admixture analysis of SNPs including *B. ashburneri* shows the same  
358 genetic cluster of *B. ashburneri* and *B. utilis* [AM] (Fig. 4b). By contrast,  
359 phylogenomic analysis based on a much larger number of SNPs shows a  
360 fully-supported monophyletic clade of *B. albosinensis* [DA], *B. ashburneri* and *B.*  
361 *utilis* [FC] (Fig. 5). The genetic similarity between *B. ashburneri* and *B. utilis* [AM]

362 based on admixture analyses of SNPs suggests *B. ashburneri* being a recent parent of  
363 *B. utilis* [AM]. This has been confirmed based on a recent phylogenomic analysis  
364 (Wang et al., 2020). In addition, gene flow between the two species may further result  
365 in genetic similarity. *Betula ashburneri* is diploid based on chromosome number and  
366 genome size analysis (Ashburner & McAllister, 2016; Wang et al., 2016), consistent  
367 with the observation that *B. albosinensis* [DA] and *B. utilis* [FC] are also diploids  
368 based on microsatellite markers. This is different from descriptions in Flora of China  
369 that *B. utilis* [FC] was a tetraploid (Li & Skvortsov, 1999). *Betula ashburneri* was  
370 described to occupy a higher altitude than *B. utilis* [AM] (McAllister & Rushforth,  
371 2011), consistent with *B. utilis* [FC] or *B. albosinensis* [DA] occupying a higher  
372 altitude than *B. utilis* ssp. *albosinensis* according to our field observations. In addition,  
373 *B. ashburneri* was discovered from SE Tibet and reported to distribute in Sichuan and  
374 Shaanxi provinces, overlapping with the distribution of *B. utilis* [FC] and *B.*  
375 *albosinensis* [DA]. Based on these, we think *B. utilis* [FC], *B. albosinensis* [DA] and  
376 *B. ashburneri* refer to the same species. *Betula ashburneri* was described to have a  
377 multi-stemmed shrubby habit and grow up to four meters in height. However,  
378 according to our field observations, it can reach 35 meters in height, consistent with  
379 descriptions from Flora of China.

380 **Cluster two — *B. costata*.**

381 Both microsatellite and SNPs indicate that *B. costata* is genetically different from  
382 other species of section *Costatae* (Figs. 3-4). Despite the fact that *B. costata* and *B.*  
383 *ermanii* co-occur in some populations, the two are morphologically different in fruit,

384 leaf and bark color. In addition, *B. costata* is a diploid and occupies a lower altitude  
385 than *B. ermanii*, which is a tetraploid.

386 **Cluster three — *B. utilis* [AM].**

387 Despite occupying a morphological continuum with *B. utilis* ssp. *albosinensis* group I,  
388 molecular results support *B. utilis* [AM] as a genetically distinct unit. *Betula utilis*  
389 [AM] are described from the Himalayas, northwestern Yunnan and with an extension  
390 into western Sichuan where it coexists with *B. utilis* ssp. *albosinensis* group I.

391 **Cluster four — *B. utilis* ssp. *albosinensis* group I.**

392 *Betula utilis* ssp. *albosinensis* group I forms a morphological continuum with *B. utilis*  
393 [AM]. However, molecular analyses indicate that *B. utilis* ssp. *albosinensis* group I  
394 forms a distinct cluster with *B. utilis* [AM] (Fig. 4b). We also found that two  
395 individuals of *B. utilis* ssp. *albosinensis* group I (XLA01 and XLA32), collected from  
396 its northern distribution, show a genetic admixture between *B. utilis* ssp. *albosinensis*  
397 and *B. ermanii* (Fig. 4b), indicating their hybrid origin. The two individuals were  
398 close to the southern distribution of *B. ermanii*, making hybridisation potentially  
399 occur due to long-distance transportation of pollen by wind. In addition, the  
400 previously described *B. albosinensis* var. *septentrionalis* and *B. utilis* var. *prattii* are  
401 more genetically similar to *B. utilis* ssp. *albosinensis* group I; however, the previously  
402 described *B. utilis* ssp. *albosinensis* is genetically similar to *B. utilis* [AM] (Fig. 4b).  
403 This indicates some misidentification of these taxa. This was suggested by  
404 observations on the very limited number of provenances in cultivation in the UK  
405 which led Ashburner and McAllister to describe these taxa as subspecies. Interestingly,

406 the included *B. albosinensis* var. *septentrionalis*, *B. utilis* var. *prattii* and *B. utilis* ssp.  
407 *albosinensis* are from Sichuan province where *B. utilis* [FC] and *B. utilis* ssp.  
408 *albosinensis* were reported to co-occur. Great morphological variations exist within  
409 some populations in Sichuan according to our field observations that even bark color  
410 within population shows substantial variation. This made assigning individuals there  
411 to either *B. utilis* ssp. *albosinensis* group I or *B. utilis* [AM] impossible based solely on  
412 morphological characters.

413 **Cluster five —*B. ermanii*.**

414 *Betula ermanii* and *B. utilis* ssp. *albosinensis* group I are genetically similar based on  
415 microsatellite markers but genetically distinct based on SNPs. This is possibly due to  
416 very recent gene flow between *B. ermanii* and *B. utilis* ssp. *albosinensis* group I.  
417 However, here we think *B. ermanii* should be recognised as a genetic unit on grounds  
418 of morphological characters and distribution. Morphologically, *B. ermanii* shows  
419 apparent differences in fruit, leaf shape, bark color and the pattern of bark peeling  
420 with *B. utilis* ssp. *albosinensis* group I. Geographically, *B. ermanii* distributes around  
421 the Changbai Mountains and its north in northeast China where *B. utilis* ssp.  
422 *albosinensis* group I is absent there.

423 **Cluster six — *B. utilis* ssp. *albosinensis* group II (*B. buggsii* as discussed below)**

424 Our genetic analyses revealed a distinct cluster of *B. utilis* ssp. *albosinensis* (group II),  
425 which was sufficiently differentiated when compared to other taxa in the genus to be  
426 ranked as a new diploid species of section *Costatae*. Based on multiple lines of  
427 evidence we describe this new species as *B. buggsii*. Molecular analyses of

428 microsatellite markers and SNPs show that *B. bugssii* is genetically distinct from all  
429 the other species of section *Costatae*. Phylogenetic analysis based on ITS sequences  
430 shows that *B. bugssii* samples cluster together despite low support values  
431 (Supplementary Data, Fig. S6). Furthermore, phylogenomic analysis including nearly  
432 genus-wide diploid species shows a fully supported monophyletic clade of *B. bugssii*,  
433 which was placed within section *Costatae* (Fig. 5). This allows us to confidently  
434 establish *B. bugssii* as a new species of section *Costatae*. Interestingly, microsatellite  
435 markers revealed two alleles at heterozygous sites for *B. bugssii* whereas three or four  
436 alleles for *B. utilis* ssp. *albosinensis*, suggesting a difference in ploidy level. Apart  
437 from these, *B. bugssii* shows morphological difference with *B. utilis* ssp. *albosinensis*  
438 in bark color and the patterns of bark exfoliation (Fig. 6a). *Betula bugssii*'s bark color  
439 is light brown and exfoliates along the elongated lenticels in stripes while *B. utilis* ssp.  
440 *albosinensis*'s bark is red and exfoliates in large sheets or flakes (Fig. 6a). The overall  
441 morphological similarity between *B. bugssii* and *B. utilis* ssp. *albosinensis* supports  
442 the placement of *B. bugssii* within section *Costatae*. Unfortunately, we failed to  
443 obtain fruiting catkins, however, we observed seedlings of *B. bugssii* in open habitats,  
444 indicating its ability to regenerate and its regeneration depends on habitat disturbance  
445 like *B. utilis* ssp. *albosinensis* (Guo et al., 2019).

446

#### 447 **A framework for species delimitation within section *Costatae***

448 A combination of various sources of information (i.e. genetic data, morphological  
449 characters, ploidy level and geographic origins) facilitates demarcating species within

450 a morphological or genetic continuum (Fig. 6b). For example, ploidy level is useful in  
451 distinguishing a species complex of differing ploidy levels. Recognition of cytotypes  
452 would help for conservation purposes as different cytotypes may have different  
453 adaptive potentials and are often genetically differentiated. If species reveals a  
454 morphological continuum, genetic data and geographic origins would help for  
455 distinguishing. This is just the case for *B. utilis* [AM] and *B. utilis* ssp. *albosinensis*  
456 group I. Similarly, for species which occupy a genetic continuum, such as *B. utilis* ssp.  
457 *albosinensis* I and *B. ermanii*, both morphological data and geographic origin aid in  
458 identification. .

459

460 Finally, for the challenging tetraploids within section *Costatae*, we propose that the  
461 most practical taxonomy is to treat populations in north-west Yunnan and the eastern  
462 and central Himalaya as *B. utilis* ssp. *utilis*; those from the Qinling Mountains as *B.*  
463 *utilis* ssp. *albosinensis*; and those from northeastern China (e.g. Changbaishan) as *B.*  
464 *ermanii*. For the diploids, it is reasonable to recognise *B. ashburneri*, *B. buggsii* and *B.*  
465 *costata* based on genetic data, morphological characters and geographic origins. The  
466 tetraploids certainly hybridise in cultivation (obser.) and so are likely to hybridise  
467 where they co-occur in the wild, generating intermediates with various levels of  
468 genetic admixture. Hence, populations collected from region between northwestern  
469 Yunnan and the Qinling Mountains may be hybrids between *B. utilis* ssp. *utilis* and *B.*  
470 *utilis* ssp. *albosinensis* and these from between Hebei and northeast China, may be  
471 hybrids between *B. utilis* ssp. *albosinensis* and *B. ermanii*. Further research is needed

472 to characterise patterns of genetic admixture between these species within their  
473 geographic distributions and to guide future management of genetic diversity.

474

475 **Acknowledgements**

476 This work was funded by the National Natural Science Foundation of China  
477 (31770230 and 31600295) and Funds of Shandong ‘Double Tops’ Program  
478 (SYL2017XTTD13).

479

480 **References**

- 481 **Abràmoff MD, Magalhães PJ, Ram SJ. 2004.** Image processing with ImageJ.  
482 *Biophotonics International* **11**: 36-42.
- 483 **Alexander DH, Lange K. 2011.** Enhancements to the ADMIXTURE algorithm for  
484 individual ancestry estimation. *BMC Bioinformatics* **12**: 246.
- 485 **Anamthawat-Jónsson K, Thórsson AT. 2003.** Natural hybridisation in birch:  
486 triploid hybrids between *Betula nana* and *B. pubescens*. *Plant Cell Tissue and*  
487 *Organ Culture* **75**: 99–107.
- 488 **Anamthawat-Jónsson K, Tómasson T. 1999.** High frequency of triploid birch  
489 hybrid by *Betula nana* seed parent. *Hereditas* **130**: 191–193.
- 490 **Andújar C, Arribas P, Ruiz C, Serrano J, Gómez-Zurita J. 2014.** Integration of  
491 conflict into integrative taxonomy: fitting hybridization in species  
492 delimitation of *Mesocarabus* (Coleoptera: Carabidae). *Molecular Ecology* **23**:  
493 4344-4361.
- 494 **Ashburner K, McAllister HA. 2016.** *The genus Betula: a taxonomic revision of*  
495 *birches*. Kew Publishing: London.
- 496 **Bacon CD, McKenna MJ, Simmons MP, Wagner WL. 2012.** Evaluating multiple  
497 criteria for species delimitation: an empirical example using Hawaiian  
498 palms (Arecaceae: *Pritchardia*). *Bmc Evolutionary Biology* **12**: 23.
- 499 **Baum DA, Small RL, Wendel JF. 1998.** Biogeography and floral evolution of  
500 Baobabs (*Adansonia*, Bombacaceae) as inferred from multiple data sets.  
501 *Systematic Biology* **47**: 181–207.
- 502 **Behr AA, Liu KZ, Liu-Fang G, Nakka P, Ramachandran S. 2016.** pong: fast  
503 analysis and visualization of latent clusters in population genetic data.  
504 *Bioinformatics* **32**: 2817-2823.
- 505 **Bickford D, Lohman DJ, Sodhi NS, Ng PKL, Meier R, Winker K, Ingram KK,**  
506 **Das I. 2007.** Cryptic species as a window on diversity and conservation.  
507 *Trends in Ecology & Evolution* **22**: 148-155.
- 508 **Bolger AM, Lohse M, Usadel B. 2014.** Trimmomatic: a flexible trimmer for  
509 Illumina sequence data. *Bioinformatics* **30**: 2114–2120.
- 510 **Bruvo R, Michiels NK, D'Souza TG, Schulenburg H. 2004.** A simple method for  
511 the calculation of microsatellite genotype distances irrespective of ploidy  
512 level. *Molecular Ecology* **13**: 2101–2106.
- 513 **Clark LV, Jasieniuk M. 2011.** POLYSAT: an R package for polyploid microsatellite  
514 analysis. *Molecular Ecology Resources* **11**: 562–566.
- 515 **DePristo MA, Banks E, Poplin R, Garimella KV, Maguire JR, Hartl C,**  
516 **Philippakis AA, del Angel G, Rivas MA, Hanna M, McKenna A, Fennell**  
517 **TJ, Kernytsky AM, Sivachenko AY, Cibulskis K, et al 2011.** A framework  
518 for variation discovery and genotyping using next-generation DNA  
519 sequencing data. *Nature Genetics* **43**: 491-498.
- 520 **Dryden IL. 2019.** shapes package. Vienna, Austria: R Foundation for Statistical  
521 Computing.
- 522 **Earl DA, vonHoldt BM. 2012.** STRUCTURE HARVESTER: a website and program



- 523 for visualizing STRUCTURE output and implementing the Evanno method.  
524 *Conservation Genetics Resources* **4**: 359-361.
- 525 **Evanno G, Regnaut S, Goudet J. 2005.** Detecting the number of clusters of  
526 individuals using the software STRUCTURE: a simulation study. *Molecular*  
527 *Ecology* **14**: 2611-2620.
- 528 **Fišer C, Robinson CT, Malard F. 2018.** Cryptic species as a window into the  
529 paradigm shift of the species concept. *Molecular Ecology* **27**: 613-635.
- 530 **Guo Y, Zhao P, Yue M. 2019.** Canopy disturbance and gap partitioning promote  
531 the persistence of a pioneer tree population in a near-climax temperate  
532 forest of the Qinling Mountains, China. *Ecology and Evolution* **9**:  
533 7676-7687.
- 534 **Hall TA. 1999.** BioEdit a user-friendly biological sequence alignment editor and  
535 analysis program for Windows 95/98/NT. *Nucleic Acids Symposium Series*  
536 **41**: 95-98.
- 537 **Hu YN, Zhao L, Buggs RJA, Zhang XM, Li J, Wang N. 2019.** Population structure  
538 of *Betula albosinensis* and *Betula platyphylla*: evidence for hybridization and  
539 a cryptic lineage. *Annals of Botany* **123**: 1179-1189.
- 540 **Jakobsson M, Rosenberg NA. 2007.** CLUMPP: a cluster matching and  
541 permutation program for dealing with label switching and multimodality in  
542 analysis of population structure. *Bioinformatics* **23**: 1801-1806.
- 543 **Jombart T. 2008.** adegenet: a R package for the multivariate analysis of genetic  
544 markers. *Bioinformatics* **24**: 1403-1405.
- 545 **Kulju KKM, Pekkinen M, Varvio S. 2004.** Twenty-three microsatellite primer  
546 pairs for *Betula pendula* (Betulaceae). **4**: 471-473.
- 547 **Leliaert F, Verbruggen H, Wysor B, Clerck OD. 2009.** DNA taxonomy in  
548 morphologically plastic taxa: Algorithmic species delimitation in the  
549 *Boodlea* complex (Chlorophyta: Cladophorales). *Molecular Phylogenetics and*  
550 *Evolution* **53**: 122-133.
- 551 **Li H. 2011.** A statistical framework for SNP calling, mutation discovery,  
552 association mapping and population genetical parameter estimation from  
553 sequencing data. *Bioinformatics* **27**: 2987-2993.
- 554 **Li H, Durbin R. 2009.** Fast and accurate short read alignment with  
555 Burrows-Wheeler transform. *Bioinformatics* **25**: 1754-1760.
- 556 **Li H, Handsaker B, Wysoker A, Fennell T, Ruan J, Homer N, Marth G, Abecasis**  
557 **G, Durbin R, Subgroup GPDP. 2009.** The sequence alignment/map  
558 format and SAMtools. *Bioinformatics* **25**: 2078-2079.
- 559 **Li PC, Skvortsov AK. 1999.** Betulaceae. Flora of China. Beijing: Science Press **4**:  
560 286-313.
- 561 **Lissambou B-J, Couvreur Thomas LP, Atteke C, Stévant T, Piñeiro R, Dauby G,**  
562 **Monthe Franck K, Ikabanga Davy U, Sonké B, M'batchi B, Hardy**  
563 **Olivier J. 2019.** Species delimitation in the genus *Greenwayodendron*  
564 based on morphological and genetic markers reveals new species. *Taxon*  
565 **68**: 442-454.
- 566 **Liu Y, Li Y, Song J, Zhang R, Yan Y, Wang Y, Du FK. 2018.** Geometric

- 567 morphometric analyses of leaf shapes in two sympatric Chinese oaks:  
568 *Quercus dentata* Thunberg and *Quercus aliena* Blume (Fagaceae). *Annals of*  
569 *Forest Science* **75**: 90.
- 570 **McAllister HA, Rushforth K. 2011.** *Betula ashburneri*. *Curtis's Botanical*  
571 *Magazine* **28**: 111–118.
- 572 **McKenna A, Hanna M, Banks E, Sivachenko A, Cibulskis K, Kernyt sky A,**  
573 **Garimella K, Altshuler D, Gabriel S, Daly M. 2010.** The Genome Analysis  
574 Toolkit a MapReduce framework for analyzing next-generation DNA  
575 sequencing data. *Genome Research* **20**: 1297-1303.
- 576 **Nagamitsu T, Kawahara T, Kanazashi A. 2006.** Endemic dwarf birch *Betula*  
577 *apoiensis* (Betulaceae) is a hybrid that originated from *Betula ermanii* and  
578 *Betula ovalifolia*. *Plant Species Biology* **21**: 19–29.
- 579 **Pritchard JK, Stephens M, Donnelly P. 2000.** Inference of population structure  
580 using multilocus genotype data. *Genetics* **155**: 945-959.
- 581 **R Core Team. 2020.** R: A Language and Environment for Statistical Computing.  
582 Vienna, Austria: R Foundation for Statistical Computing.
- 583 **Rosenberg NA. 2004.** DISTRUCT: a program for the graphical display of  
584 population structure. *Molecular Ecology Notes* **4**: 137-138.
- 585 **Salojärvi J, Smolander O-P, Nieminen K, Rajaraman S, Safronov O, Safdari P,**  
586 **Lamminmäki A, Immanen J, Lan T, Tanskanen J, Rastas P, Amiryousefi**  
587 **A, Jayaprakash B, Kammonen JI, Hagqvist R, et al 2017.** Genome  
588 sequencing and population genomic analyses provide insights into the  
589 adaptive landscape of silver birch. *Nature Genetics* **49**: 904-912.
- 590 **Stamatakis A. 2006.** RAxML-VI-HPC: maximum likelihood-based phylogenetic  
591 analyses with thousands of taxa and mixed models. *Bioinformatics* **22**:  
592 2688–2690.
- 593 **Thomson AM, Dick CW, Pascoini AL, Dayanandan S. 2015.** Despite  
594 introgressive hybridization, North American birches (*Betula* spp.) maintain  
595 strong differentiation at nuclear microsatellite loci. *Tree Genetics &*  
596 *Genomes* **11**: 101.
- 597 **Truong C, Palmé AE, Felber F, Naciri-Graven Y. 2005.** Isolation and  
598 characterization of microsatellite markers in the tetraploid birch, *Betula*  
599 *pubescens* ssp. *tortuosa*. *Molecular Ecology Notes* **5**: 96-98.
- 600 **Tsuda Y, Semerikov V, Sebastiani F, Vendramin GG, Lascoux M. 2017.**  
601 Multispecies genetic structure and hybridization in the *Betula* genus across  
602 Eurasia. *Molecular Ecology* **26**: 589–605.
- 603 **Tsuda Y, Ueno S, Ide Y, Tsumura Y. 2009.** Development of 14 EST-SSRs for *Betula*  
604 *maximowicziana* and their applicability to related species. *Conservation*  
605 *Genetics* **10**: 661-664.
- 606 **Wang N, Borrell JS, Bodles WJA, Kuttapitiya A, Nichols RA, Buggs RJA. 2014a.**  
607 Molecular footprints of the Holocene retreat of dwarf birch in Britain.  
608 *Molecular Ecology* **23**: 2771–2782.
- 609 **Wang N, Borrell JS, Buggs RJA. 2014b.** Is the Atkinson discriminant function a

- 610 reliable method for distinguishing between *Betula pendula* and *B.*  
611 *pubescens* (Betulaceae)? *New Journal of Botany* **4**: 90-94.
- 612 **Wang N, Kelly LJ, McAllister HA, Zohren J, Buggs RJA. 2020.** Resolving  
613 phylogeny and polyploid parentage using genus-wide genome-wide  
614 sequence data from birch trees. *bioRxiv*:  
615 <https://doi.org/10.1101/2020.1107.1113.200444>.
- 616 **Wang N, McAllister HA, Bartlett PR, Buggs RJA. 2016.** Molecular phylogeny and  
617 genome size evolution of the genus *Betula* (Betulaceae). *Annals of Botany*  
618 **117**: 1023-1035.
- 619 **Wang N, Thomson M, Bodes WJA, Crawford RMM, Hunt HV, Featherstone AW,**  
620 **Pellicer J, Buggs RJA. 2013.** Genome sequence of dwarf birch (*Betula*  
621 *nana*) and cross-species RAD markers. *Molecular Ecology* **22**: 3098-3111.
- 622 **White TJ, Bruns T, Lee S, Taylor T. 1990.** Amplification and direct sequencing of  
623 fungal ribosomal RNA genes for phylogenetics *PCR protocols: a guide to*  
624 *methods and applications*. New York: Academic press: 315-322.
- 625 **Whittall JB, Hellquist CB, Schneider EL, Hodges SA. 2004.** Cryptic species in an  
626 endangered pondweed community (*Potamogeton*, Potamogetonaceae)  
627 revealed by AFLP markers. *American Journal of Botany* **91**: 2022-2029.
- 628 **Wu B, Lian C, Hogetsu T. 2002.** Development of microsatellite markers in white  
629 birch (*Betula platyphylla* var. *japonica*). *Molecular Ecology Notes* **2**: 413-415.
- 630 **Zohren J, Wang N, Kardalsky I, Borrell JS, Joecker A, Nichols RA, Buggs RJA.**  
631 **2016.** Unidirectional diploid-tetraploid introgression among British birch  
632 trees with shifting ranges shown by restriction site-associated markers.  
633 *Molecular Ecology* **25**: 2413-2426.

634

635

636 **Figure legends**

637 **Figure 1** The distribution of samples used in the present study.

638 **Figure 2** (a) Principal component analysis (PCoA) of leaves of section *Costatae*  
639 species. (b) ‘Eigenleaves’ showing leaf morphs represented by principal components  
640 (PCs) at  $\pm 3SD$  and shape variance explained by each PC. Each dot represents a leaf.

641 **Figure 3** Principal coordinate analysis (PCO) of section *Costatae* species at 15  
642 microsatellite markers (a) and principal component analysis (PCoA) of section  
643 *Costatae* species at 82,137 SNPs (b).

644 **Figure 4** STRUCTURE results of section *Costatae* at K values 5 and 6 based on 15  
645 microsatellite markers (a) and admixture analysis of section *Costatae* at K values 5  
646 and 6 at the 82,137 SNPs (b).

647 **Figure 5** Species tree from the maximum likelihood analysis of the diploid *Betula*  
648 species using the supermatrix approach based on data from 2,285,620 SNPs.  
649 Bootstrap support values of 100 were not shown. Numbers on the branches are  
650 bootstrap support values between 60 and 100. The scale bar below indicates the mean  
651 number of nucleotide substitutions per site. Species were classified according to Wang  
652 et al. (2020).

653 **Figure 6** A schematic illustration of species delineation within section *Cosatate* (a)  
654 and various sources of information used to distinguish species (b). Photos of each  
655 species were placed below its names.

656 **Figure S1** Principal coordinate analysis (PCO) of section *Costatae* species at 15  
657 microsatellite markers (a) and principal component analysis (PCoA) of section

658 *Costatae* species at 82,137 SNPs (b).

659 **Figure S2** The best number of clusters inferred using “Evanno test” method.

660 **Figure S3** STRUCTURE results of section *Costatae* at K values from 2 to 6 based on  
661 15 microsatellite markers.

662 **Figure S4** The cross-validation error for each K value from 1 to 10.

663 **Figure S5** Admixture results at K values from 2 to 10 based on 82,137 SNPs.

664 **Figure S6** Phylogenetic tree from the maximum likelihood analysis of *B. bugssii*  
665 using ITS sequences. Species were classified according to Ashburner and McAllister  
666 (2016). Values above branches are bootstrap percentages of >50 %.

667 **Table legends**

668 **Table 1** Detailed information on taxa of section *Costatae* used in the present study.

669 **Table S1** Detailed information on populations used in the present study.

670 **Table S2** Details of microsatellite primers used in the present study.

671 **Table S3** Detailed information of samples used for ITS and RAD sequencing.

672

673

674

675

676

677

678

679

680

681

682

683

684

685 **Table 1** Detailed information on taxa of section *Costatae* used in the present study.

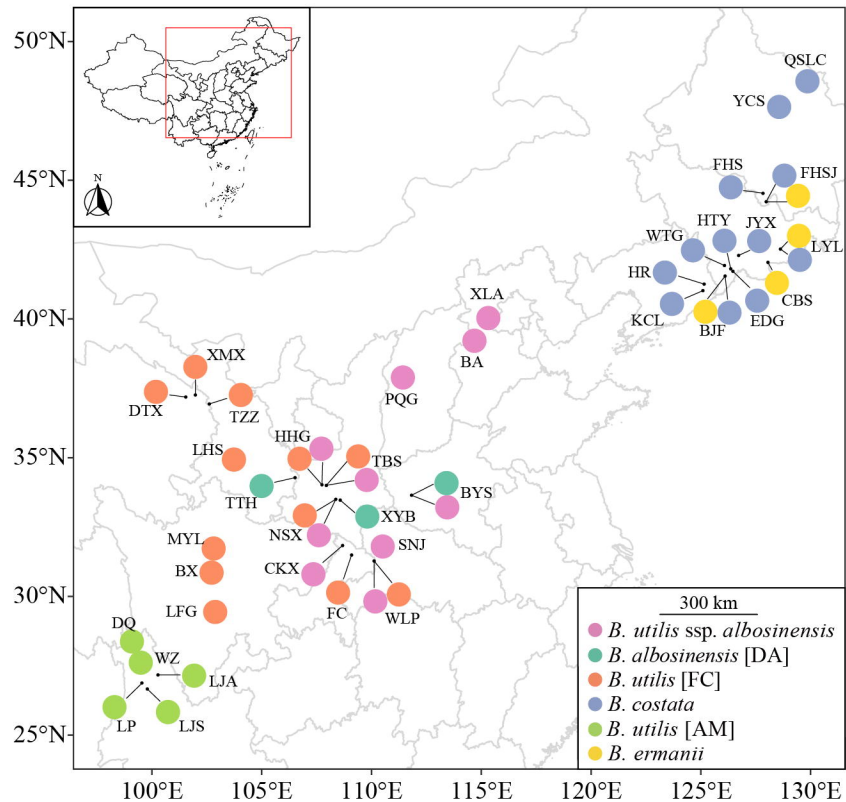
Species	Variety	Ploidy	Distribution	Reference
<i>B. utilis</i>	<i>ssp. utilis</i>	tetraploid	Nepal, eastwards through SE Tibet to Yunnan and west Sichuan where it merges with <i>ssp. albosinensis</i>	Ashburner and McAllister, 2016
	<i>ssp. utilis</i>	tetraploid	Gansu, Hebei, Ningxia, Qinghai, Shaanxi, west Sichuan, E and S Xizang, NW Yunnan	Li and Alexei, 1999, Flora of China
	<i>var. pratii</i>	tetraploid	Kangding, western Sichuan	Ashburner and McAllister, 2016
	<i>ssp. albosinensis</i>	tetraploid	North Sichuan, Hubei, south Gansu, south Ningxia, south Shaanxi, Shanxi, Henan and Hebei	Ashburner and McAllister, 2016
	<i>ssp. albosinensis</i>	diploid	south Shaanxi	Hu et al., 2019
<i>B. albosinensis</i>	<i>ssp. septentrionalis</i>	tetraploid	Western Sichuan	Ashburner and McAllister, 2016
<i>B. ermanii</i>	<i>ssp. ermanii</i>	tetraploid	Northeast China, Japan, Korea and the Russian Far East	Ashburner and McAllister, 2016
	<i>var. lanata</i>	tetraploid	Russia: from the eastern shores of Lake Baikal, eastward to the Pacific coast except Korea and north China	Ashburner and McAllister, 2016

---

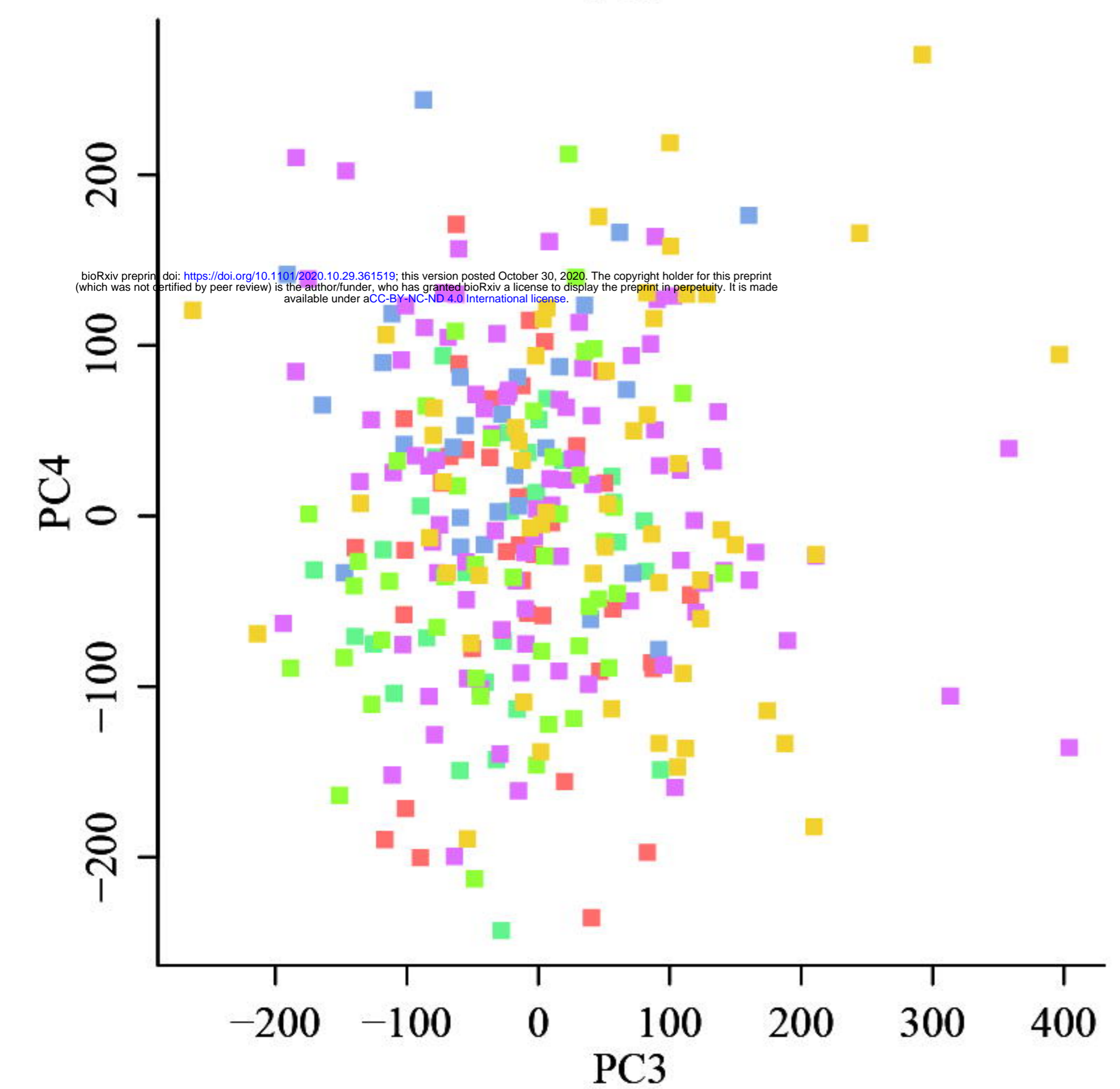
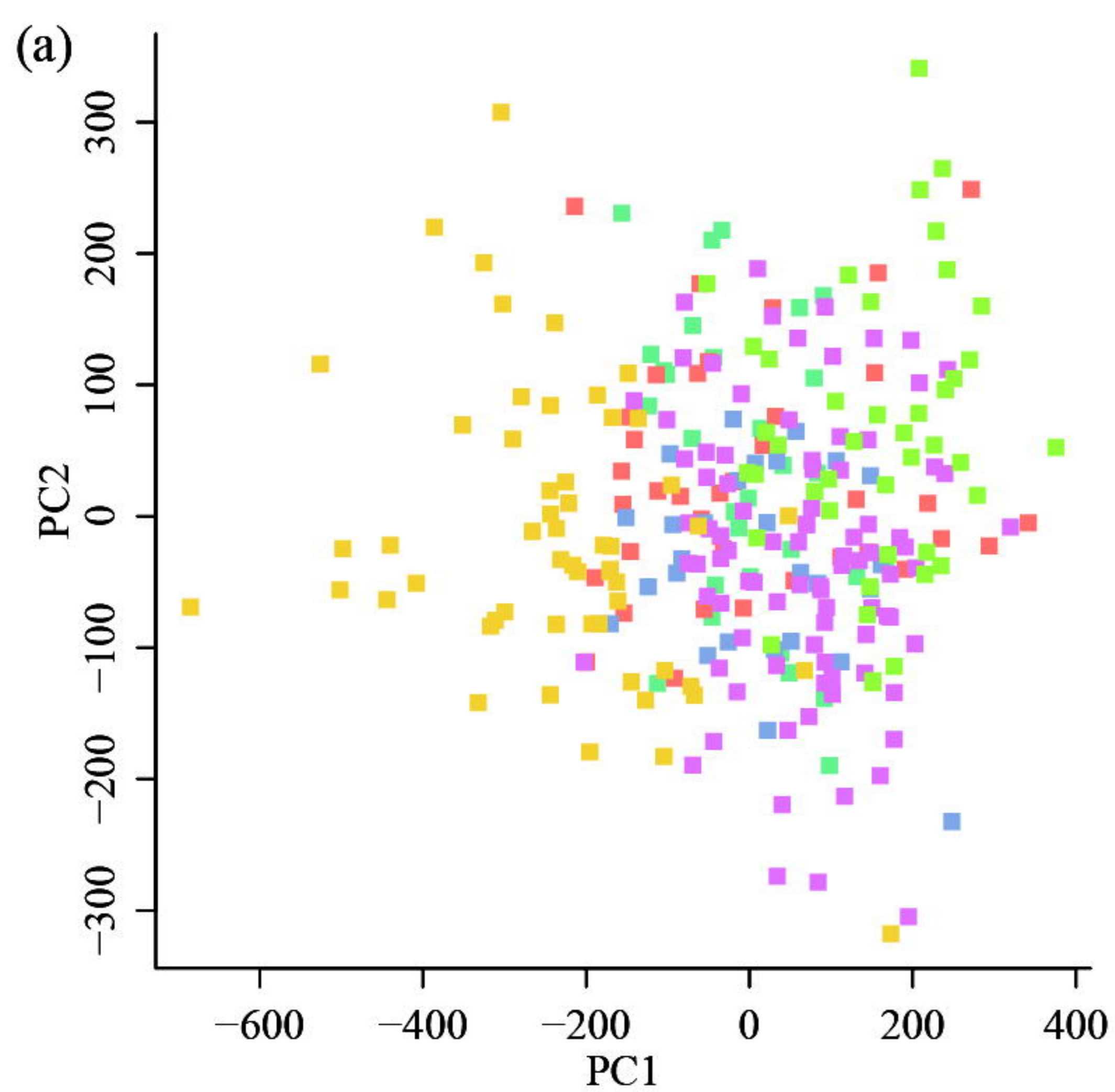
<i>B. costata</i>	NA	diploid	Northeast China	Ashburner and McAllister, 2016
<i>B. ashburneri</i>	NA	diploid	Southeast Tibet, Northwest Yunnan, Southwest Sichuan and possibly Shaanxi	McAllister, 2011; Ashburner and McAllister, 2016

---

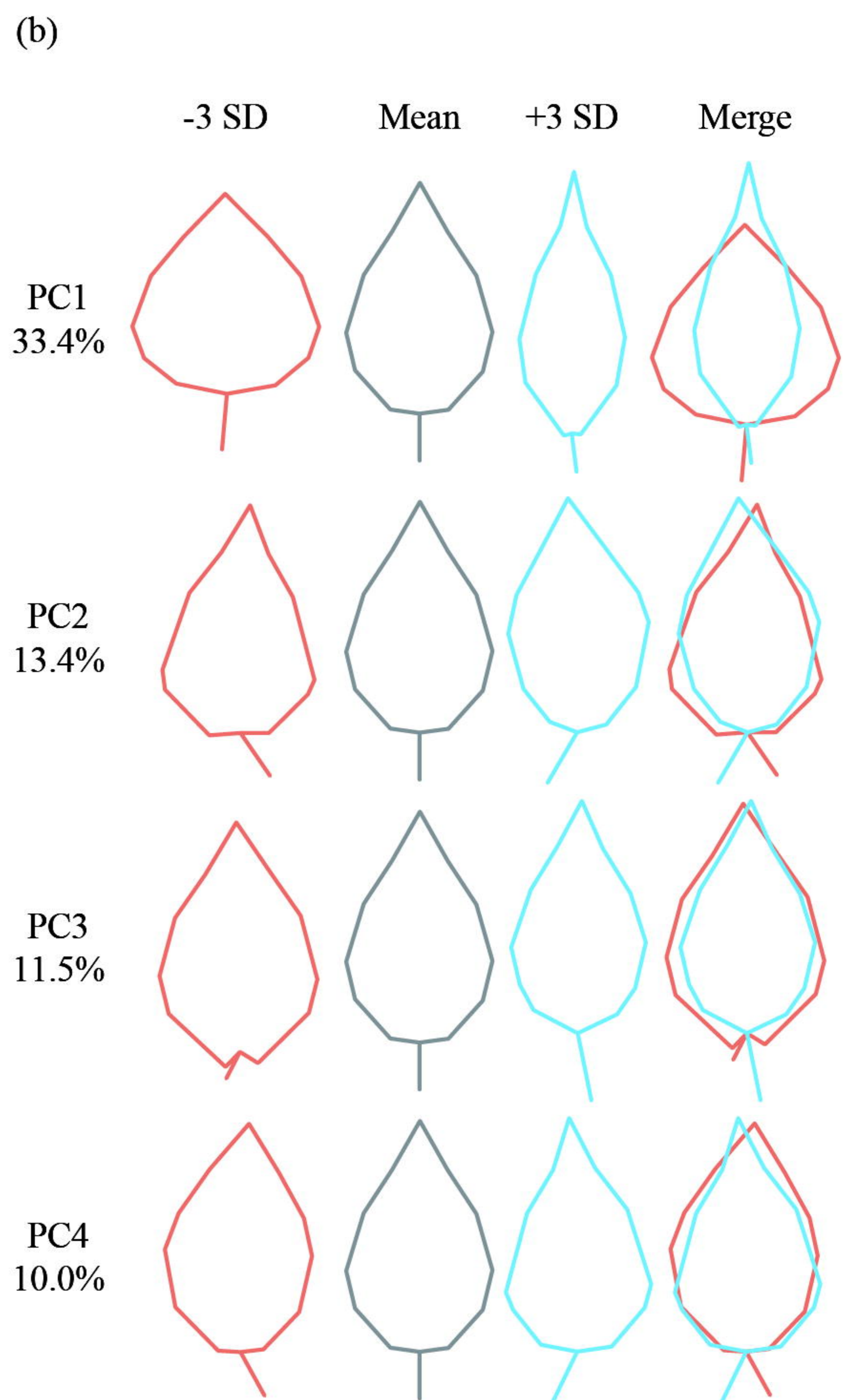
686

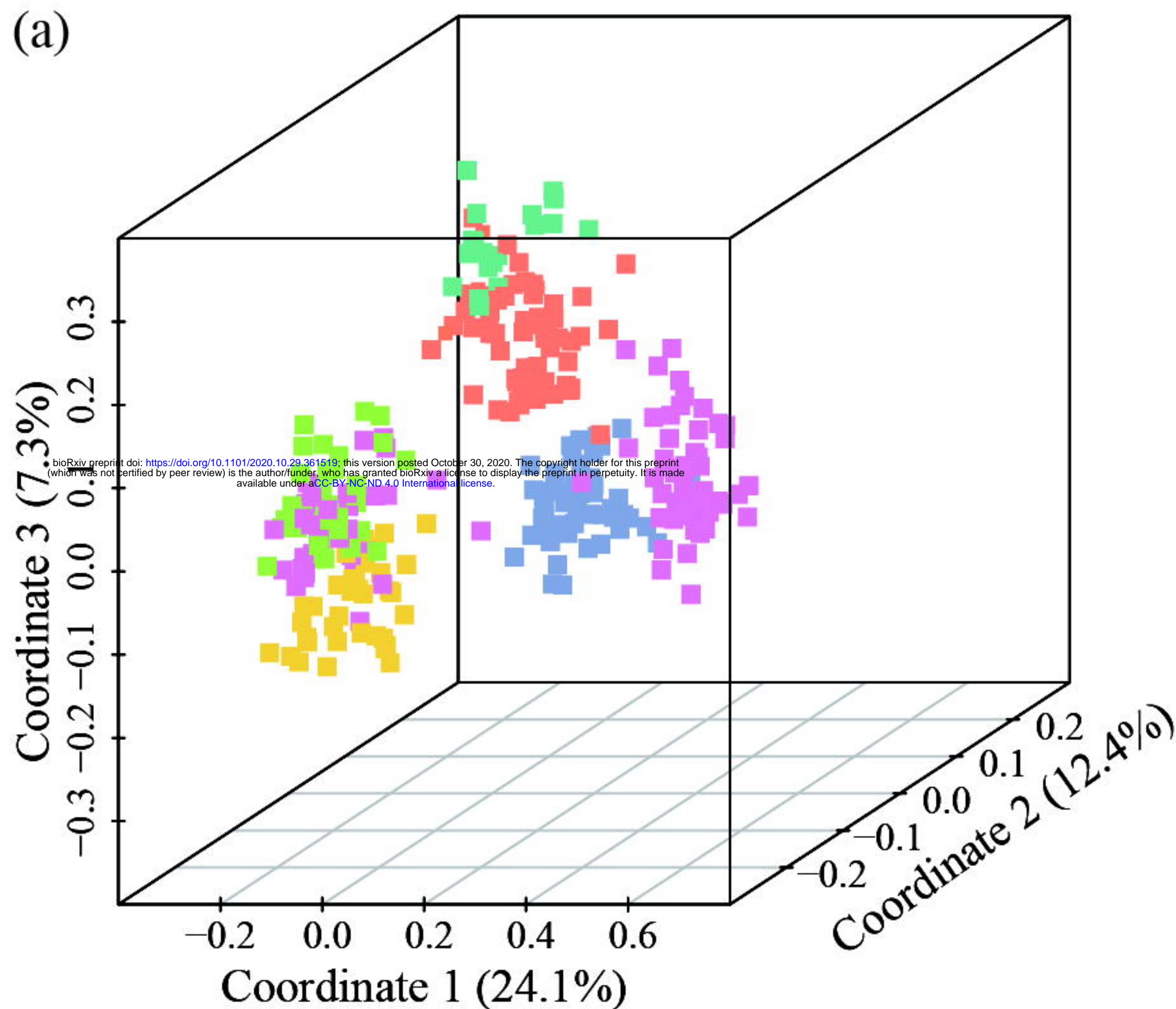




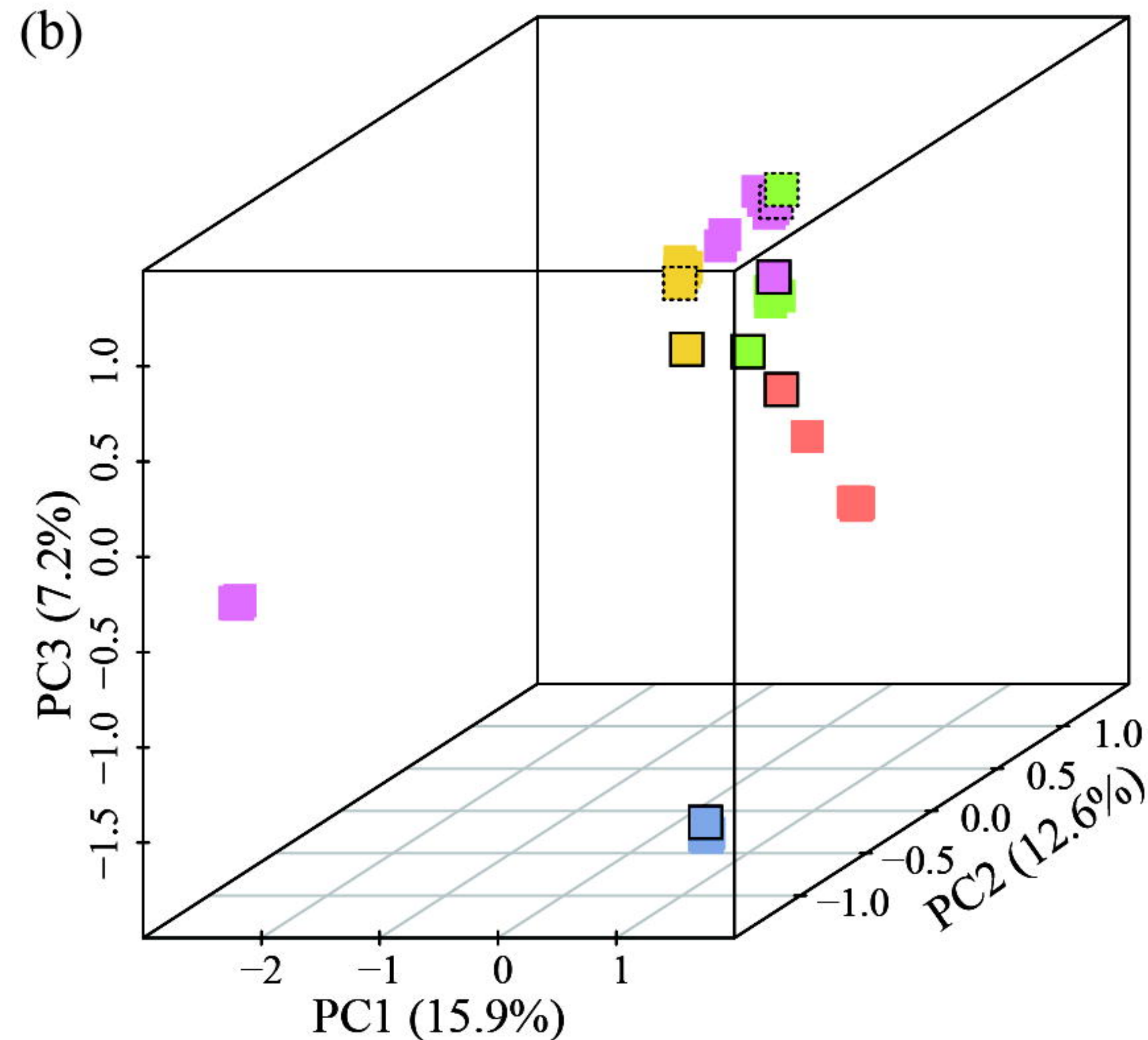


■ *B. utilis ssp. albosinensis*     ■ *B. costata*  
■ *B. albosinensis* [DA]     ■ *B. utilis* [AM]  
■ *B. utilis* [FC]     ■ *B. ermanii*





■ *B. utilis* ssp. *albosinensis*  
■ *B. albosinensis* [DA]  
■ *B. utilis* [FC]  
■ *B. costata*  
■ *B. utilis* [AM]  
■ *B. ermanii*



■ *B. ashburneri*  
■ *B. costata*  
■ *B. utilis* ssp. *utilis*  
■ *B. ermanii*  
■ *B. albosinensis* var. *septentrionalis*  
■ *B. utilis* var. *prattii*  
■ *B. ermanii* var. *lanata*

